

## **The natural relation between prestack time migration and residual statics analysis**

Xinxiang Li and John Bancroft

### **ABSTRACT**

In terms the purpose of data processing, conventional residual statics analysis methods are essentially trying to correct randomly distributed traveltimes errors on seismic traces for the best possible stacked section. On the other hand, in terms of residual statics analysis, CMP stacking is the essential process for conventional methods to provide reference traces with less traveltimes errors.

Prestack migration also contains a stacking process after proper time correction. The scattered energy on different traces from a scatter point will be aligned in time. The migration stacking process sums these time-corrected traces and produces the time imaging of the scatter point.

From migrated traces, an inverse migration process can be applied to produce multi-offset reference data volume. The stacking processes in both migration and its inverse (de-migration) involve much more traces than NMO plus CMP stacking, and statistically attenuate traveltimes errors more efficiently. Unfortunately, prestack migration (especially depth migration) is more velocity sensitive than NMO plus CMP stacking process.

Equivalent offset migration (EOM) introduces an intermediate step for prestack time migration, which is a constant time mapping from source-receiver offset to migration equivalent offset. This equivalent offset mapping, also as a stacking process, reduces the traveltimes error effects. An inverse mapping from equivalent offset back to source-receiver offset can be applied to form a set of reference traces.

Comparing to the full prestack migration and its inverse (de-migration), the main advantages of the forward and inverse equivalent offset mappings are:

- (1) No time shift is involved in the process, which avoids time direction distortion, such as NMO stretch.
- (2) It is velocity insensitive, and practically no velocity information is needed.
- (3) It is computationally more efficient.

Plausible results have been obtained from the application of residual statics analysis based on the reference model data created by equivalent offset mapping.

### **INTRODUCTION**

Before emphasizing on the relations among residual statics analysis, NMO plus CMP stacking and prestack migration, some reviews and comments are presented in this introduction. First, a short summary of general methods of residual statics analysis is presented. And then some concepts relevant to prestack migration are

reviewed. Specifically, the kinematics of equivalent offset migration (EOM) method (Bancroft and et al, 1995) is stated, because it is used to form a new method for residual statics analysis.

### Principle of residual statics analysis

Most of the algorithms for surface consistent residual statics analysis follow a procedure that can be simply expressed as following steps (also shown in Figure 1):

- Step1: Using the reflection information on seismic traces, where the traveltimes might be distorted by the near surface effects, to form traces (they are called reference traces or model traces) which are assumed having less effects from near surface anomalies.
- Step2: Comparing each seismic trace and its corresponding reference trace to estimate their traveltime difference.
- Step3: Decompose the time differences estimated on each seismic trace into surface consistent (and sub-surface consistent) source statics and receiver statics.

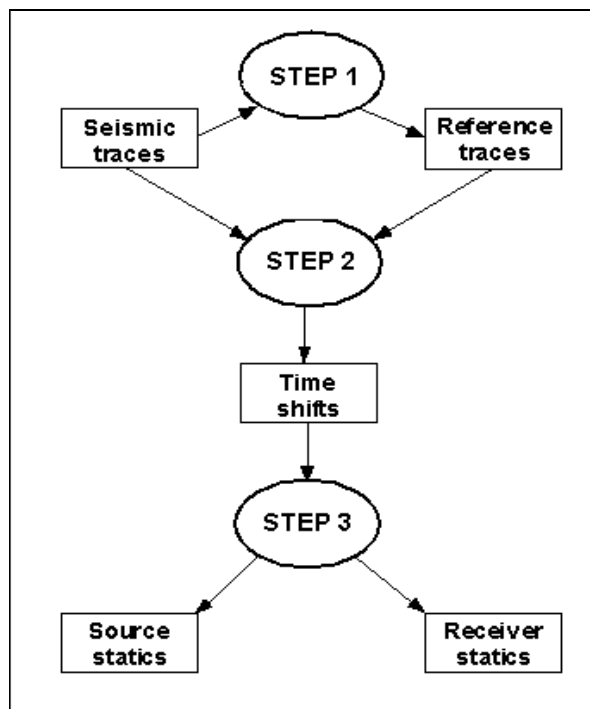


Figure 1: General three-step procedure for residual statics analysis methods.

In this three-step scheme, the starting point is the seismic reflection data itself. The reference model data is formed in the first step and then both the seismic traces and the reference traces are inputted to Step 2 to estimate the traveltime on seismic traces. These traveltime errors may not be geophysically reasonable, so Step 3 is usually used to estimate surface consistent source and receiver statics. In each step, different algorithms can be used and it theoretically does not influence the performance of other steps.

The three steps are also closely related to each other for some specific algorithms. If the reference traces are formed without NMO correction involved, then the decomposition for surface consistent statics should not contain the term related to NMO errors. The stack-power maximization method (Ronen and Claerbout, 1985) combines Step 2 and Step3 by forming super traces within shot and receiver gathers.

Most of the recent developments in residual statics analysis present new ways to form more reliable reference data, Larner (1998) and Chan and Stewart (1996,1997) are the typical examples.

### The scatter point model for prestack migration

In seismic data processing, the subsurface of the earth is often modeled as a layered medium with each layer having uniform acoustic properties. The reflection energy from the interfaces can be considered as the superposition of the scattered energy from a large number of “closely” spaced points on the interfaces. The reflection amplitude at each point is taken as proportional to the reflection coefficient of the interface at this point. This “sampled” subsurface model is called scatter point model, which forms the basis of Kirchhoff migration method. In addition, the points that may not locate at any recognizable interface can be considered as scatter points with zero or very small reflection amplitudes.

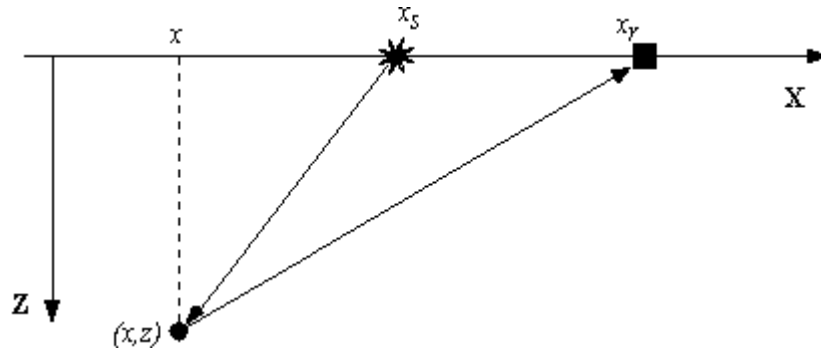


Figure 2: The geometry of a scatter point. A scatter point scatters incoming energy back in any direction. The wave propagation velocity is assumed to be constant.

Assuming that the propagation velocity for seismic waves in the subsurface is a constant  $V$ , for any scatter point located at  $(x, z)$ , and any pair of surface source and receiver located at  $x_s$  and  $x_r$ , the traveltime of seismic waves from the source to the scatter point then to the receiver can be expressed as (see Figure 2)

$$T = \frac{1}{V} \cdot \left[ \sqrt{z^2 + (x_s - x)^2} + \sqrt{z^2 + (x_r - x)^2} \right] \tag{1}$$

The two-way vertical traveltime  $\tau$ , which equals to  $2 \cdot \frac{z}{V}$ , is equivalent to depth  $z$  when the velocity is constant. It is also the traveltime when the source and the receiver both locate at the surface location of the scatter point, i.e.,  $x_s = x_r = x$ .

Relation (1) can be expressed as following by replacing  $z$  with  $\tau$ ,

$$T = \sqrt{\frac{\tau^2}{4} + \frac{(x_s - x)^2}{V^2}} + \sqrt{\frac{\tau^2}{4} + \frac{(x_r - x)^2}{V^2}}. \quad (2)$$

In the Kirchhoff approach of time migration, a point on a migrated time section,  $(x, \tau)$ , is often considered as a scatter point. Although the extension of scatter point concept from depth domain to two-way vertical time domain is not perfect when velocity varies, equation (2) can well approximate the traveltime response of a scatter point for most of the cases when the subsurface structure is not very complex. In fact, the migration velocity for time imaging at a time domain scatter point  $(x, \tau)$  is actually defined by equation (2) in terms of collecting most amount of diffracted energy from the corresponding depth domain scatter point.

Equation (2) is often called the double-square-root (DSR) equation, and it can be expressed in CMP and offset domain as

$$T = \sqrt{\frac{\tau^2}{4} + \frac{(x_{off} - h)^2}{V^2}} + \sqrt{\frac{\tau^2}{4} + \frac{(x_{off} + h)^2}{V^2}}. \quad (3)$$

where  $x_{cmp}$  denotes a CMP surface location,  $h$  denotes the half source-receiver offset and  $x_{off}$  denotes the surface lateral distance between a CMP location and the scatter point  $(x, \tau)$ .

In 3-D  $(x_{off}, h, T)$  space, this equation describes a 2-D surface called Cheop's pyramid (Claerbout, 1985).

### Kinematics of equivalent offset migration (EOM)

EOM is based on prestack Kirchhoff time migration, with an intermediate step forming prestack migration gathers at each migration output location. The gathers are sorted by a new offset measure called equivalent offset. The equivalent offset  $h_e$  is defined by converting the DSR equation (3) into an single square root form, and this is geometrically accomplished by defining a pair of collocated "source" and "receiver" such that the traveltime keeps the same. That is

$$\sqrt{\frac{\tau^2}{4} + \frac{(x_{off} - h)^2}{V^2}} + \sqrt{\frac{\tau^2}{4} + \frac{(x_{off} + h)^2}{V^2}} = T = 2 \cdot \sqrt{\frac{\tau^2}{4} + \frac{h_e^2}{V^2}}.$$

From this relation, the equivalent offset  $h_e$  can be explicitly expressed as

$$h_e^2 = h^2 + x_{off}^2 - \frac{4x_{off}^2 h^2}{V^2 T^2}. \quad (4)$$

The migration gathers formed by the mapping from source-receiver offset to equivalent offset are called common scatter point (CSP) gathers. The full migration is then completed by moveout correction (NMO) and CDP stacking applied to each of these CSP gathers.

## PRESTACK MIGRATION AND RESIDUAL STATICS ANALYSIS

Automatic residual statics analysis has original relation with NMO correction plus CMP stacking process, while prestack time migration in many ways can be considered as an extension to the NMO plus stacking. This implies a natural relation between migration and residual statics analysis.

### NMO correction and CMP stacking

#### *Relation with Residual statics analysis*

Many conventional methods of residual statics analysis compare NMO corrected traces with their corresponding CMP stacked traces to obtain estimates of the possible traveltime errors on these traces. In these methods, the CMP stacked traces are used as the references of the NMO corrected traces instead of the original seismic traces before NMO correction. This relation between NMO plus stacking (shorted as NMOPS) process and residual statics analysis is illustrated in Figure 3.

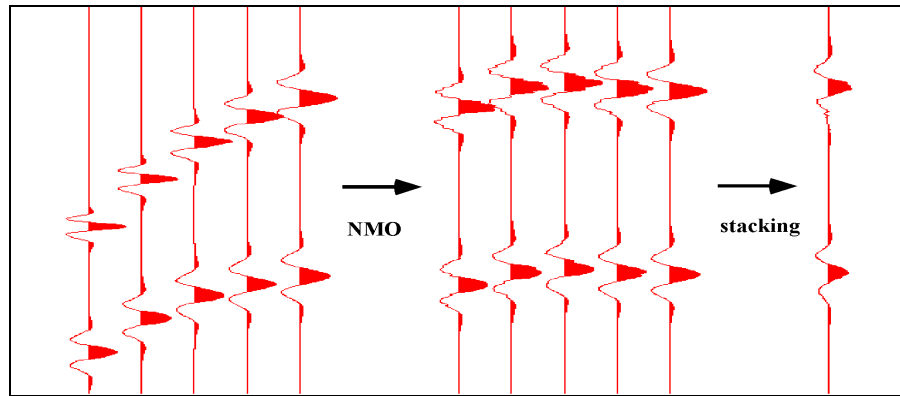


**Figure 3:** Many conventional residual statics analysis methods can be essentially interpreted as a comparison technique between CMP stacked traces with the NMO corrected traces (before stacking) to estimate the possible time differences.

It is reasonable to consider that the stacked traces can “equivalently” be used as the references for the original pre-NMO traces if we properly remove the NMO correction from stacked traces. NMO correction as a deterministic time-shift operation can be approximately reversed by its inverse (INMO). Therefore, for each seismic trace in a CMP gather, its reference trace can be formed by apply INMO on the stacked trace with proper offset and velocity information, which should be the information used to NMO correct the seismic trace. This process is illustrated in Figure 4.

This NMOPS+INMO approach for building reference traces at least has two advantages. First, the inverse NMO corrected reduce the effects caused by the inaccuracy of the NMO velocities. The second, the decomposition process from the estimated traveltime errors to the surface consistent source and receiver statics will be less effected by the residual NMO terms, which also does not have deterministic solutions.

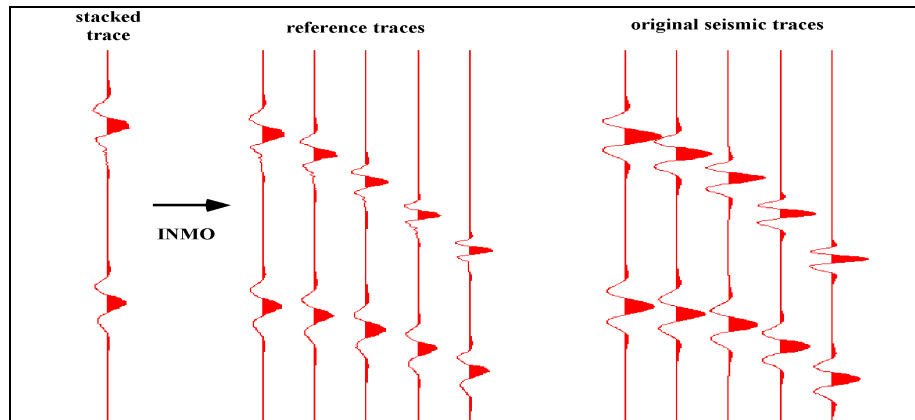


**Figure 4:** Residual statics can also be estimated by comparing the original seismic traces (before NMO) with the offset dependent INMO-ed stacked traces. NMO and INMO should use the same velocity function.

Unfortunately, because INMO can not exactly reverse the NMO operation applied on seismic traces, and the inaccuracy involved with NMO correction can usually be reasonably removed by proper approximation of the RNMO errors during statics estimation, the INMO step in practice seems unnecessary.

For the purpose of forming reference trace to estimate residual statics, it is the statistical property of CMP stacking process that attenuates the traveltime random errors. The NMO correction, as a deterministic process, is used only because it is required for CMP stacking. If there are other methods that can also utilize the stacking property to reduce the random effects of traveltime errors, NMO may not be necessary.

#### *Relation with prestack time migration*

NMOPS process and prestack time migration have similar properties and many differences in many aspects.

First, these two processes can both be decomposed into moveout correction and stacking. The moveout correction in migration process can be called migration moveout (MMO) correction contrast to NMO, and the stacking process after MMO can be called CSP stacking for contrasting to CMP stacking process. The stacking processes in both migration and NMOPS sum the time-shifted traces together and located them at the expected output locations.

Reflection events on NMO corrected traces in a CMP gather are assumed aligned cross the offset direction, thus the CMP stacking process is mainly a technique to enhance the signal. MMO corrected traces for certain CSP location are also assumed similar to each other in the way that the samples at the same time may come from the same scatter point. The CSP stacking process can then be considered as a signal enhancement tool, and it cancels random time errors on the traces.

Second, NMO correction of a sample on a seismic trace is determined by the source-receiver offset of the trace and the velocity information at related CMP

location. While MMO correction of a sample is determined by its equivalent offset. The equivalent offset is not only related to the source-receiver offset and the velocity information at the output location, but also changes with the lateral distance between the CMP location and the output CSP location.

The third, in NMOPS, each input trace only contributes to one output location, and only one NMO correction is applied on this trace. In migration process, an input seismic trace theoretically contributes to all the output CSP locations, and different MMO corrections have to be applied for different output locations (Figure 5).

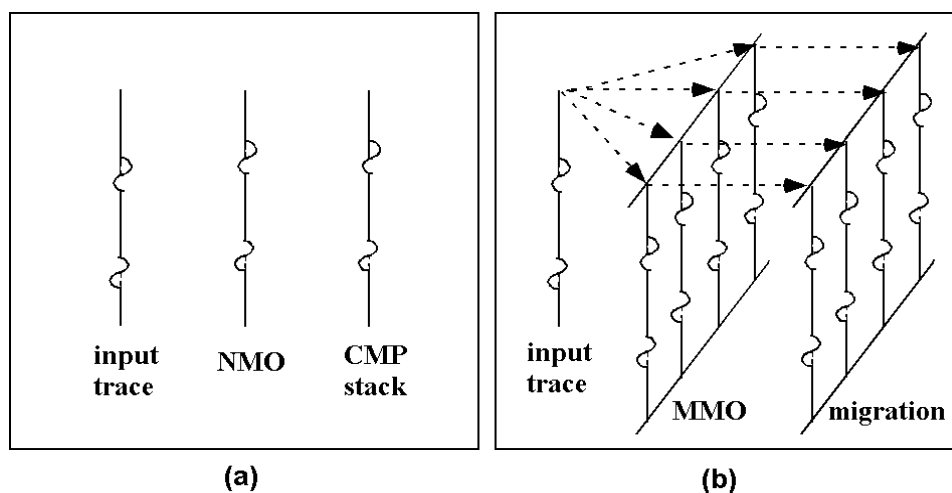


Figure 5: The difference between the energy contributions of an input trace to the output data of NMOPS and prestack time migration. (a) In the NMOPS process, one input trace is NMO corrected only once and it contributes to only one trace in the stacked section. (b) In prestack time migration, theoretically, an input trace will contribute to all the migration output locations, and for each contribution, a new MMO correction should be applied to this trace.

The fourth, for a trace in CMP stacked sections, the total number of traces contributed to this stacked trace is the fold of the present CMP gather, which is usually not greater than 100. While for a trace in migrated time sections, theoretically all the traces in the prestack data volume have contributions to this migrated trace (Figure 6).

In addition, when the migration velocity function and NMO velocity function are the same at some surface location, then the NMO-stacking process is just part of the migration process. Because for each trace at the CMP gather at this location, its contribution to the CMP stacked trace and its contribution to the migrated trace at this location are exactly the same.

These similarities and differences between NMOPS and prestack migration imply that prestack migration is an extension of NMOPS, some applications related to NMOPS, such as residual statics analysis, can be naturally related to prestack time migration.

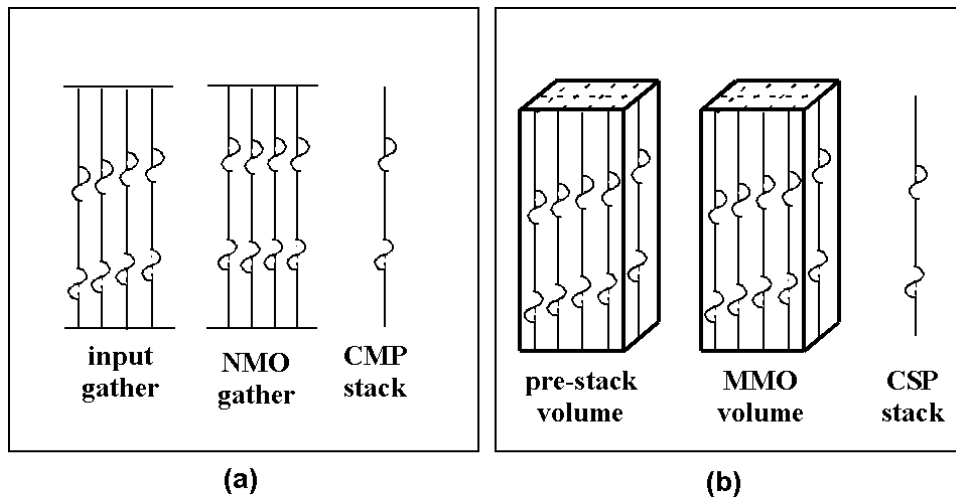


Figure 6: The difference between CMP stacked traces and the migrated traces in terms of collecting energy from input prestack data volume. (a) A CMP stacked trace collects only the energy from one CMP gather, while (b) a migrated traces contains energy from all the traces in related migration aperture, and theoretically can be all the traces in the volume.

**Prestack migration provides reference model for residual statics analysis**

Similar to NMOPS followed by an offset dependent INMO, which forms reference model traces for residual statics analysis, prestack migration, including MMO and CSP stacking, can also form statics reference data by introducing an equivalent offset dependent inverse MMO (IMMO). This IMMO process can also be called de-migration because it tends to remove the effects of migration. This migration plus de-migration method can be illustrated as a flow chart in Figure 7.

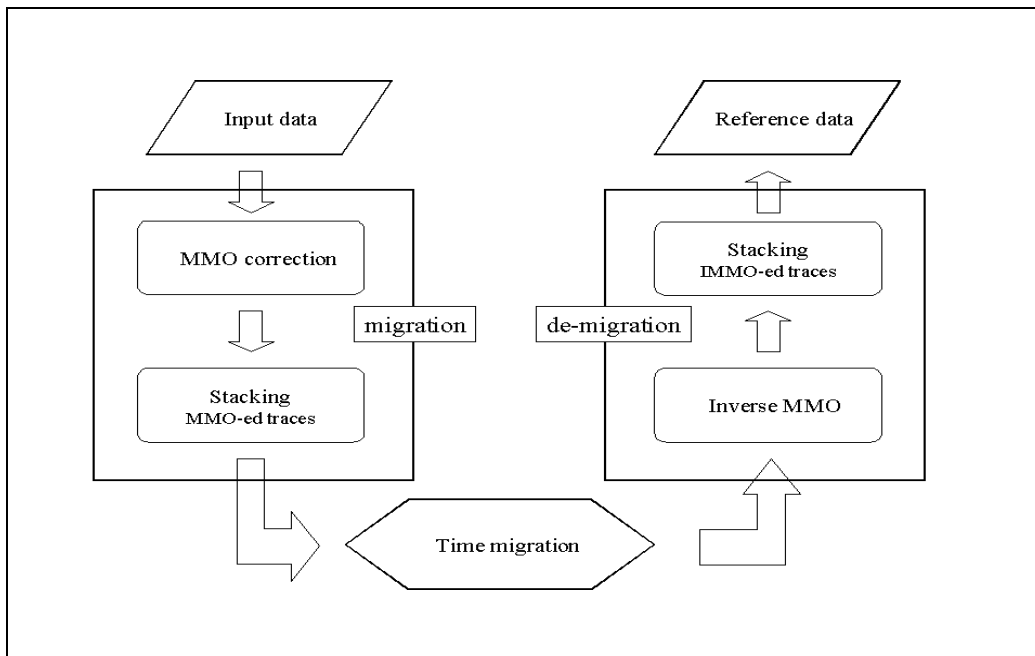


Figure 7: Prestack time migration and its inverse (de-migration) can form model data as the reference for residual statics analysis.

In terms of forming model data with less travelttime errors, migration plus de-migration process has some advantages over NMOPS plus INMO. The migration stacking process involves much more traces, and it should statistically do a better job on attenuation of the travelttime errors, at least it is not influenced by the very low fold CMP gathers, where travelttime error may not be attenuated at all. In addition, the de-migration process also including a stacking process of the IMMO-ed traces.

This migration related process also has disadvantages. Migration process involves much more traces from larger surface range, so its stacking process may have more chances to introduce errors due to inaccurate MMO corrections on these traces.

The accuracy of migration moveout (MMO) correction mainly depends on the accuracy of migration velocities, which are even more difficult to observe than NMO stacking velocities. The migration velocity dependence restricts the practical application of migration plus de-migration method to form reference traces for statics analysis. Lerner (1998) suggested that, the migration plus de-migration process can be used to improve the observation of both residual statics and migration velocity in an iterative manner.

**EOM provides a better way: migration equivalent offset mapping**

Full migration plus de-migration process with EOM concept can interpret the method shown in Figure 7 as a detailed process in Figure 8.

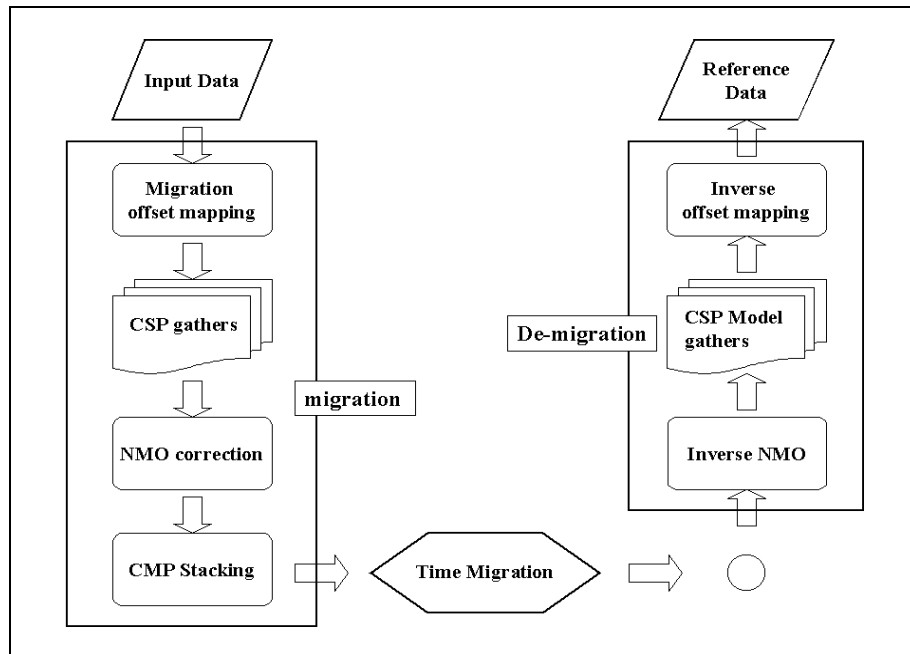


Figure 8: Full migration and de-migration processes with CSP gathering as the intermediate step. Notice that, a set of “model” CSP gathers is constructed in the flow.

It is noticed that, a set of “model” CSP gathers is constructed during the process shown in Figure 8, which is obtained by apply multi-offset INMO on migrated traces. In fact, these model CSP gathers can be directed replaced by the CSP gathers formed in the migration process. Because as a stacking process, the forward migration offset

mapping (from source-receiver offset to equivalent offset) can very well attenuate the traveltime random errors, and the CSP gathered traces already contain much less effects from the near surface anomalies. Besides, the mapping from equivalent offset back to source-receiver offset (inverse offset mapping) will further reduce the effects from random traveltime errors.

Thus, the flow chart in Figure 8 can be very much simplified by ignoring the NMOPS and its inverse process applied on CSP gathers. A new flow for constructing statics reference traces is shown in Figure 9.

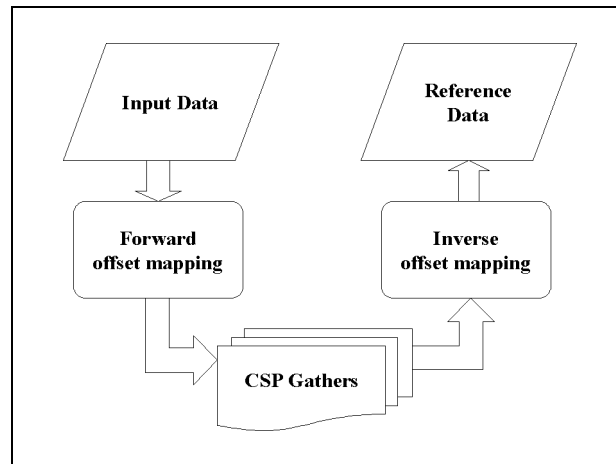


Figure 9: Reference traces for residual statics analysis can be more efficiently built by using just the forward and inverse equivalent migration offset mappings. Moveout correction and its inverse are excluded.

This new approach is not only more efficient than the ones shown in Figure 8 and Figure 7, it also excludes the traveltime moveout correction process. This is good especially for residual statics analysis as moveout correction may very possibly distort the statics. In addition, the approach has another very important advantage that the whole process shown in Figure 9 is not velocity sensitive. For the purpose of forming residual statics reference data, practically no velocity information is needed.

## VELOCITY DEPENDENCE ANALYSIS

As mentioned above, the migration and de-migration processes can form better reference traces for residual statics analysis, as long as we can have reasonably accurate migration velocity information. The scheme in Figure 9 is more feasible because it is a process that very in-sensitive to migration velocity errors. In this section, some detailed analysis of the velocity dependence of equivalent offset mapping is shown and some totally velocity independent approximations of the migration equivalent offset mapping are presented.

### Velocity sensitivity

In the definition of equivalent offset, i.e., equation (4),  $T$ ,  $h$  and  $x_{off}$  are usually accurate, so the equivalent offset error is usually due to the error of migration velocities. The sensitivity of the equivalent offset error versus the velocity error can

be expressed as the ratio of the relative error of equivalent offset to the relative velocity error (Bancroft and Geiger, 1995), i.e.,

$$S(h_e, V) = \left| \frac{dh_e/h_e}{dV/V} \right| = \left| 1.0 - \frac{x_{off}^2 + h^2}{h_e^2} \right| = \frac{4x_{off}^2 h^2}{h_e^2 V^2 T^2} . \quad (5)$$

And because  $\max(|x_{off}|, |h|) \leq \frac{1}{2}VT$ ,  $h_e \geq \max(|x_{off}|, |h|)$  and  $h_e \leq \sqrt{x_{off}^2 + h^2}$ , the sensitivity is always limited as  $S(h_e, V) \leq 1$ . This means when the velocity error is 10%, the relative error of the equivalent offset can not be greater than 10%. In fact, the following detail analysis tells that the sensitivity is usually much smaller. In some cases, the errors can practically be ignored.

Instead of directly giving the values of the sensitivity, the relative equivalent offset errors are shown in terms of input velocity relative errors in the following analysis. The relative input velocity errors change from  $-100\%$  to  $100\%$ , where the minimum wrong velocity is half the accurate velocity and the maximum wrong velocity is twice the accurate velocity.

The sensitivity is a function of four variables, they are the migration distance  $x_{off}$ , the half source-receiver offset  $h$ , the traveltime  $T$  and the accurate migration velocity  $V$ . Because  $x_{off}$  and  $h$  are symmetric in expression (5), the following results show the behavior of sensitivity versus  $x_{off}$ ,  $T$  and  $V$ .

#### *Sensitivity changing with migration distance $x_{off}$*

Figure 10A shows some curves for different migration distances  $x_{off}$ , and each curve represents relative equivalent offset error as a function of the percentage of the velocity errors at one distance  $x_{off}$ . While for all the curves, the half source-receiver offset  $h$  is equal to 500 meters; the accurate velocity  $V$  is 3000 meters per second and the traveltime  $T$  is 1.0 second. The migration distance  $x_{off}$  is sampled from 0 to  $0.5VT=1500$  meters by every 200 meters.

It is noticed that, the sensitivity, which is the ratio of relative equivalent offset error to the corresponding relative velocity error, is less than 0.2 in this case. And, there is significant difference between the sensitivity of higher velocity and lower velocity. In this example, when input velocity changes from 3000 m/s down to 1500 m/s, the equivalent offset goes down 18%, while the input velocity goes up from 3000 m/s to 6000 m/s, the equivalent offset is less than 4% more than the accurate value. This suggests that, when the accurate velocity is known between two velocities, use the higher one as input will usually give better results.

Figure 10B shows only the equivalent error values for those velocities that are higher than the accurate one, i.e., the positive percentages of the velocity errors. It is just part of the Figure 10A. The later analysis will only show the results with higher wrong velocities.

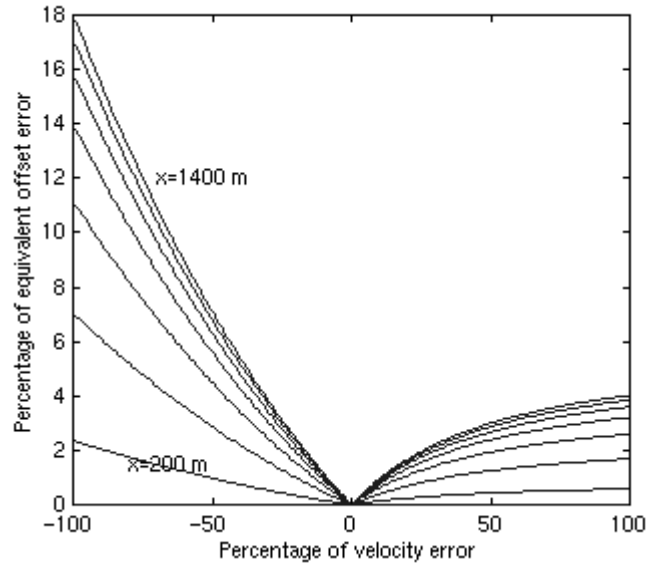


Figure 10A: Relative equivalent offset error versus relative velocity error shown as curves for different migration distances  $x_{off}$ . The  $h$  is 500 meters,  $V$  is 3000 meters per second and  $T$  is 1.0 second, and  $x_{off}$  is sampled from 0 to 1500 meters by every 200 meters.

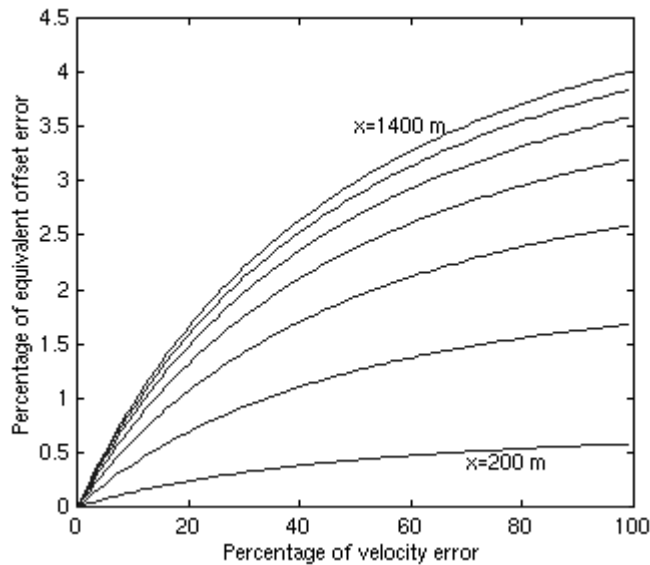


Figure 10B: This is part of Figure 10A with only the relative equivalent offset error curves at positive velocity error percentages are shown.

For fixed  $h$ ,  $T$  and  $V$ , the sensitivity of equivalent offset error versus input velocity error usually increases with migration distance  $x_{off}$ . This increasing also relies on the value of  $h$ .

*Sensitivity versus travelttime  $T$*

Figure 11 shows some equivalent offset error curves for different travelttime  $T$ . As in Figure 10B, only the values at positive percentage velocity errors are shown. For

all the curves,  $x_{off}$ ,  $h$  and the accurate velocity  $V$  are known as 600 meters, 500 meters and 3000 meters per second.

The sensitivity of equivalent offset error versus input velocity error decreases as the traveltime  $T$  increases. From Figure 11, it decreases very rapidly at the first one second or so, from 2.6% down to 0.6% at 100% wrong velocity. Usually, for data after three seconds, the error due to traveltime is practically zero. This means, the equivalent offsets of the samples with traveltime larger than 3 seconds, the velocity error does not practically result in significant differences. This is very useful at least for forming residual statics reference data when no velocity information is available.

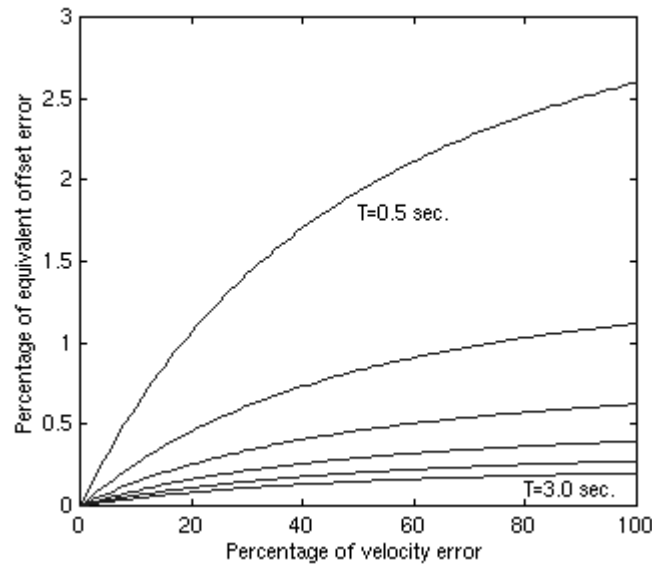


Figure 11: Relative equivalent error curves for different traveltime  $T$ s. The half offset  $h$  is still 500 meters, the migration distance  $x_{off}$  is now fixed at 600 meters, the accurate velocity  $V$  is still 3000 m/s.  $T$  is now sampled from 0.5 to 3.0 seconds by every 0.5 second.

#### *Sensitivity versus accurate velocity $V$*

Figure 12 shows some equivalent offset error curves for different accurate migration  $V$ 's. For all these curves,  $x_{off}$ ,  $h$  and  $T$  are fixed at 600 meters, 500 meters and 1.0 second respectively.

The sensitivity of equivalent offset error versus input velocity error decreases as the migration velocity  $V$  increases. For example, in Figure 12, when the accurate migration velocity is 2000 m/s, if 4000 m/s (100% error) is used, the equivalent offset will be 6% more than the accurate value. While if the accurate velocity is 4000 m/s, an 8000 m/s (also 100% error) velocity is used, the equivalent offset will be only 1.1% more than the accurate value.

As a summary, for a given trace with fixed source-receiver offset  $2h$ , when the migration distance  $x_{off}$  is small relative to  $h$ , the traveltime of the samples are large and the accurate migration velocity is large, then velocity (larger than accurate) error may not be a serious problem, at least for forming statics reference data.

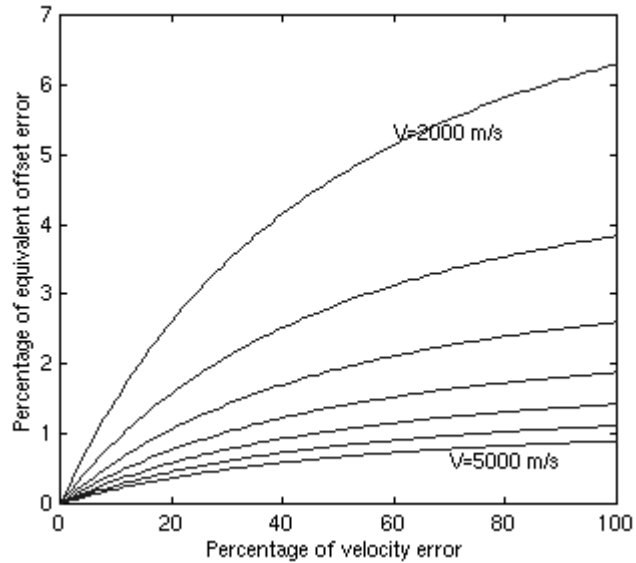


Figure 12: Relative equivalent offset error curves versus relative velocity errors for different accurate migration  $V$ . The half offset  $h$  is 500 meters, the migration distance  $x$  is 600 meters, the traveltime  $T$  is 1.0 second. Velocity  $V$  is now sampled from 2000 to 5000 m/s with 500 m/s increment. Only the curves at positive percentage velocity errors are shown.

### Total velocity independence: the asymptotic offset mappings

The equivalent migration offset mappings are based on the definition of the equivalent offset  $h_e$ , i.e. equation (4). For any  $x_{off}$  and  $h$ , when the traveltime  $T$  of a sample is very large relative to any other quantities, then  $h_e$  tends to equal  $h_{e\omega}$  as

$$h_{e\omega} = \sqrt{x_{off}^2 + h^2} \quad (5)$$

We call this  $h_{e\omega}$  asymptotic equivalent offset. This also tells that the time slice of Cheop's pyramid tends to be a square in migration distance and half source-receiver offset ( $x_{off}, h$ ) space, and the properties of this square is not only independent to the traveltime, it also independent to the velocity. Figure 13 shows the contour of a Cheop's pyramid at different times. Practically, at relative later time, the equivalent offset can be approximated by its asymptotic version, which is totally independent to velocity and traveltime.

In fact, this asymptotic equivalent offset is accurate at ant traveltime for some cases. From the definition of the equivalent offset, when either offset  $h$  or migration distance  $x_{off}$  equals to zero, the asymptotic equivalent offset is equal to the accurate one. This implies that, when  $h$  is small relative to  $x_{off}$ , or  $x_{off}$  is small relative to  $h$ , or in other words, when  $x_{off}$  or  $h$  is small relative to the equivalent offset, the asymptotic equivalent offset can be a good approximation to the accurate solution even at early times. This property of migration equivalent offset mapping is also very important for the application of forming statics reference data when velocity information is unknown. The direct suggestion is using small migration aperture (distance) limit.

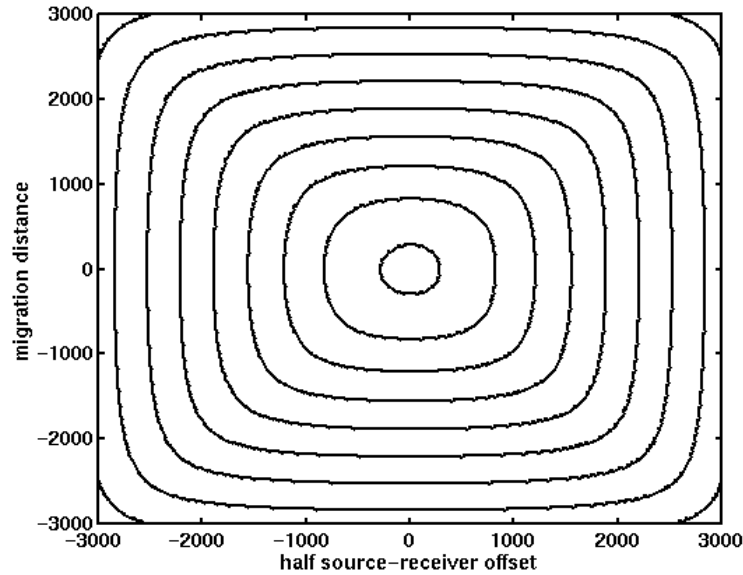


Figure 13: Contours of a Cheop’s pyramid at different time. The corresponding scatter point is located at two-way time 0.8 second, the related velocity is 2000 m/s, and the time levels are from 0.85 second to 3.4 seconds with 0.3 second as the increment. The contours tend to be a square as the time increases.

There is another explanation of the definition of the asymptotic equivalent offset. For a sample at any finite traveltime  $T$ , if the migration velocity  $V$  tends to be infinite, the corresponding equivalent offset also tends to be the asymptotic equivalent offset, and finally becomes traveltime independent.

In practice, velocity cannot be infinite, but the maximum possible velocity can always be estimated for any seismic experiment. Also, there is always a maximum traveltime in any seismic data. By these two “maximum” quantities, a better approximation for equivalent offset can be formed, and it is velocity and traveltime independent.

$$h_{em}^2 = h^2 + x^2 - \frac{4x^2 h^2}{V_{max}^2 T_{max}^2}, \quad (6)$$

where  $V_{max}$  is the maximum possible migration velocity and  $T_{max}$  is the maximum traveltime on seismic traces. We call this new approximation pre-asymptotic equivalent offset.  $h_{em}$  is always a better approximation to  $h_e$  than  $h_{e\omega}$ , because the relation between  $h_e$ ,  $h_{e\omega}$  and  $h_{em}$ , i.e.,  $h_e^2 \leq h_{em}^2 \leq h_{e\omega}^2$  always holds. In some cases, especially when travel time  $T$  is not large, there can be some significant differences between  $h_{e\omega}$  and  $h_{em}$ .

## SYNTHETIC DATA EXPERIMENTS

### Reliability of the method

The first experiment shown here is the application of equivalent offset mapping method to a set of synthetic data where no traveltime errors are involved. The expected solution should only contain zeros for both source and receiver statics.

The subsurface model contains only two flat reflectors. The acquisition geometry is designed as shown in Figure 14. This geometry ensures that both source and receiver folds (source fold 161 and receiver fold 41) are evenly high through the entire line. The synthetic data is 4 millisecond sampled.

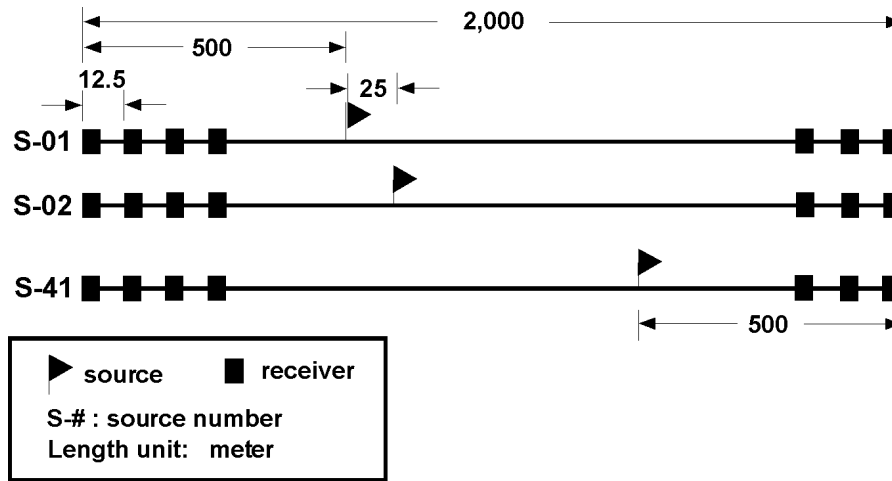


Figure 14: Geometry of a set of synthetic data. All the receivers (total number of 161) are activated for each shot (total number of 41). The line begins at 0 and end at 2,000 meters where the first and the last receivers are located respectively. The receiver interval is 12.5 meters. The shot interval is 25 meters. The first shot locates at 500 meters and the last locates at 1500 meters.

The synthetic data has no traveltime errors on its traces. The migration equivalent offset mapping method (CSP method for short) is applied to this data, and as expected, the source and receiver statics obtained are very close to zero. Figure 15 shows the results, where the upper part is the source statics, which are less than 0.06 millisecond. The lower part shows the receiver statics, whose absolute values are less than 0.35 millisecond. The average absolute value of the source statics is 0.02 millisecond, and the average absolute value of the receiver statics is 0.096 millisecond. Comparing to the sample rate of the data, these statics are virtually zero.

The direct conclusion from the results in Figure 15 is that, if there is no traveltime errors on the seismic traces, the equivalent offset mapping method gives zero values for the statics. Thus, this method is reliable for obtain statics solution.

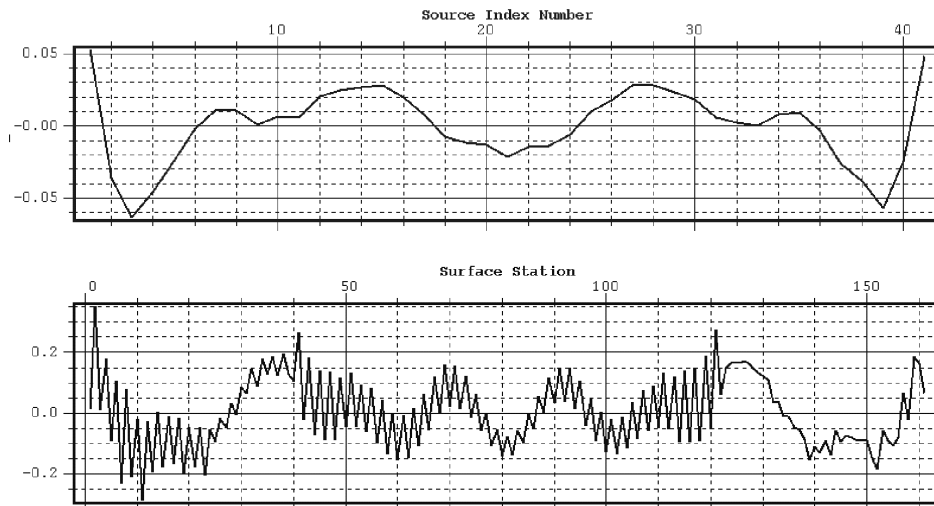


Figure 15: The statics solution for synthetic data without any traveltim errors. The upper part shows the estimated source statics, which is numbered by the source index number. The lower part shows the estimated receiver statics, which is numbered by receiver surface locations. The source statics (absolute value) are less than 0.06 millisecond and the receiver statics (absolute value) are less than 0.35 millisecond.

The reliability of each value of the statics at certain locations can be quantified by the maximum value of the cross-correlation function. Figure 16 shows the maximum values (it can be called confidence) of normalized cross-correlation functions during the comparison between the synthetic seismic traces and their reference model traces created by our equivalent offset method. They are very close to 1.0 (with an average 0.93), and ensure the high similarity between the synthetic seismic traces and their corresponding reference traces.

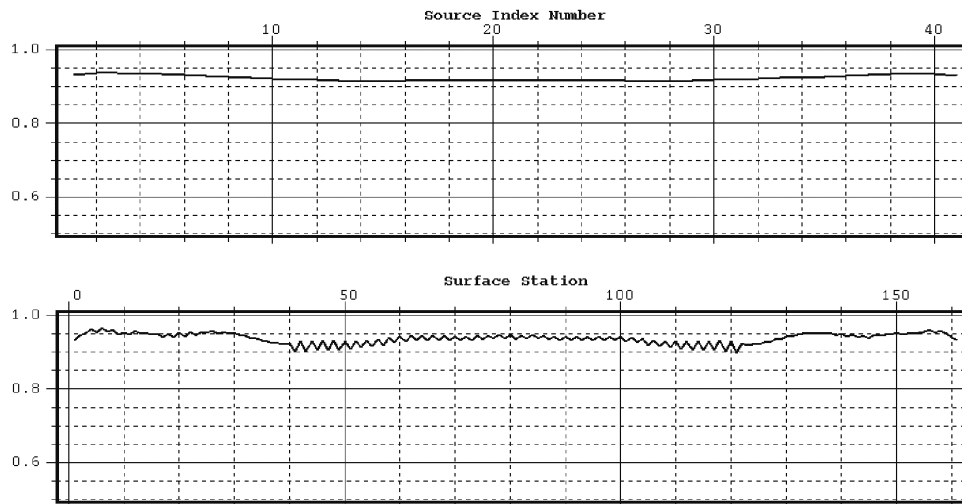


Figure 16: The confidence of the source and receiver statics shown in Figure 15.

### Geometry consideration

The synthetic data used for previous experiment is acquired using the geometry shown in Figure 14, where all 161 receivers are activated for all 41 sources. The shot

gathers and receiver gathers have very high fold. This not only increases the reliability of the reference traces, but also enhances the accuracy of the decomposed surface consistent statics.

For comparison, using the same subsurface 2-reflector model, but with an acquisition layout shown in Figure 17, a new set of synthetic data is acquired. The source fold keeps a constant value 81, while the receiver fold changes from 1 to 41, as shown in figure 18.

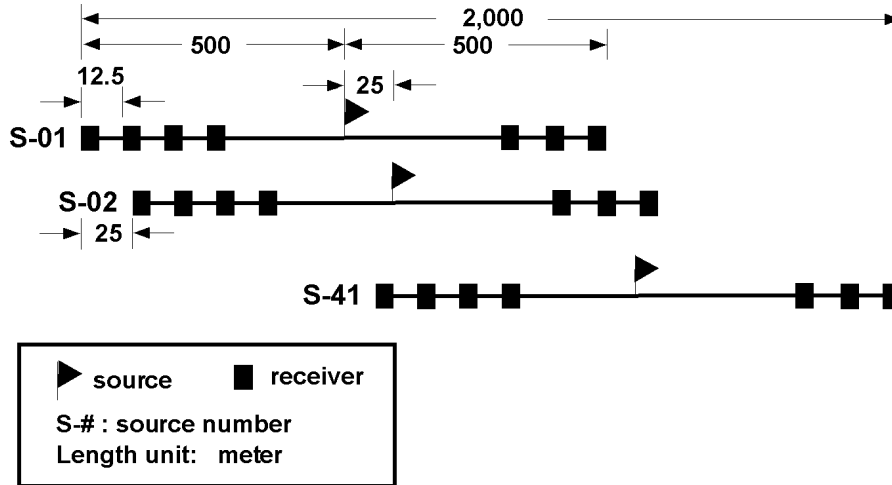


Figure 17: Geometry of another set of synthetic data. Different from the geometry shown in Figure 14 (where the receiver fold is constant 41), the fold of the common receiver gathers changes from 1 to 41.

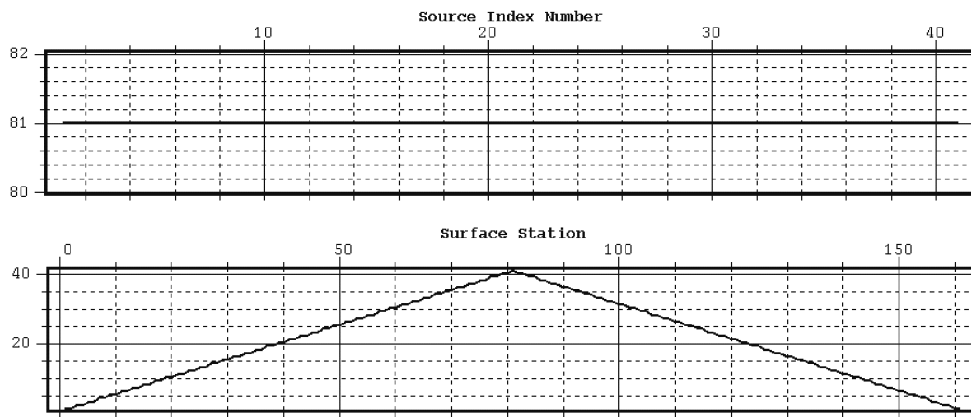


Figure 18: The source fold (top) and the receiver fold (low) of the synthetic data acquired using geometry shown in Figure 17.

The source statics may not be influenced very much because the fold for each shot gather is still evenly high. While the receiver statics may not be very reliable at those locations where the receiver fold is very low. The statics are shown in Figure 19. As expected, the error (related to the expected zero value) in source statics are still less than 0.1 millisecond (the seismic traces are sampled by 4 milliseconds). While the error in receiver statics is now relatively larger than the estimates shown in Figure 15.

But the locations where the error is more than 0.4 millisecond only located at the two ends of the line, where the receiver fold is no more than 3.

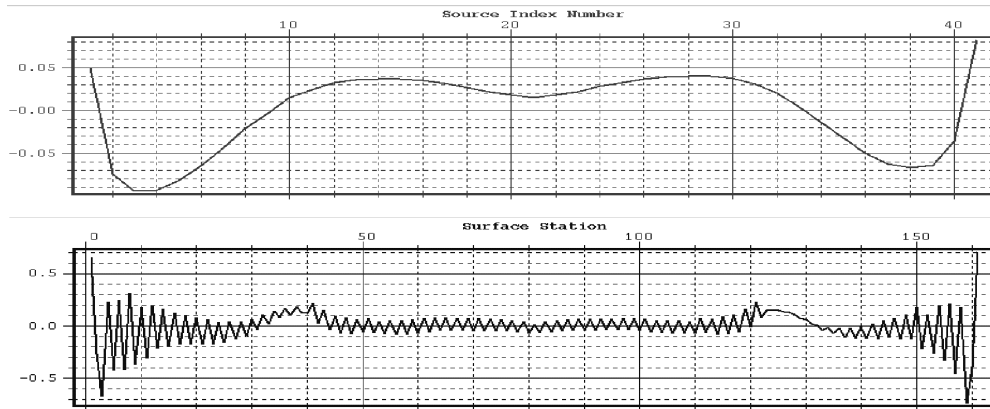


Figure 19: The statics estimated by CSP statics analysis method from the data acquired from the geometry shown in Figure 17. The source statics are limited between  $-0.09$  to  $0.08$  millisecond, and the receiver statics are limited between  $-0.7$  to  $0.7$  millisecond. The errors (related to the expected zero value) are still practically ignorable.

In addition, the symmetry of the spread also helps the reliability of the statics. The influences from the asymmetry of the spread can be seen from the receiver statics estimates in both Figure 15 and Figure 19. At the ends of the seismic lines, the spread of each receiver becomes less symmetric than it is in the middle of the line, and as a result, the statics errors at the ends of the line are relatively larger.

It is important to mention that, all the results in the two experiments did not involve any velocity analysis, the forward and inverse equivalent offset mappings actually used the asymptotic equation (5), where no velocity information is needed.

### Traveltime error attenuation

For the demonstration of how the forward and inverse migration equivalent offset mappings attenuate the traveltime errors, some synthetic random time shifts are applied to the synthetic data with the geometry shown in Figure 17, where the receiver fold changes along the line.

The synthetic statics is applied in a surface consistent manner, this means for one source or receiver location, there is one time shift amount for all the traces in the source or receiver gathers. The source shifts and the receiver shifts are limited within the range of  $-12$  ms to  $12$  ms. So the largest possible shift applied on a trace is about 48 ms.

Figure 20 shows one shot gather (left) and its reference gather (right) formed by equivalent offset mapping and its inverse. Also, the offset mappings are using the asymptotic equation (5). The traveltime errors on the shot gather are recognizable on both reflection events. It can be seen that, the events on the reference shot gather are much smoother, even though there are still some non-continuity.

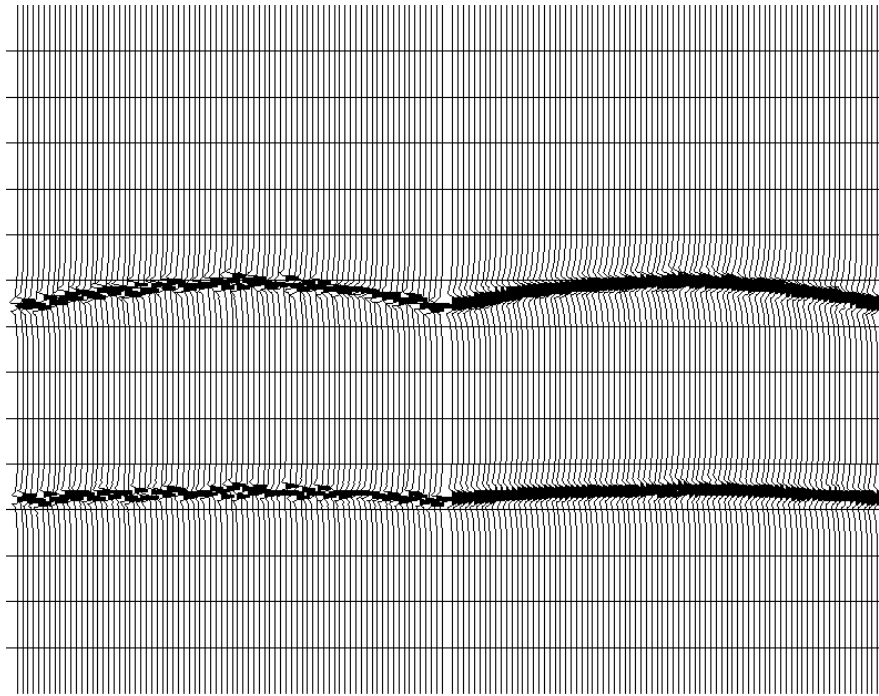


Figure 20: A synthetic shot gather with some random time shift applied (left) and its reference gather (right) created by using forward and inverse asymptotic equivalent offset mappings where no velocity information is required.

Due to the “smearing” effects in the offset mapping stacking process, it is noticed that the dominant frequency of the reference traces is lower than the original traces. But this does not influence very much to the comparison between a trace and its reference trace to only estimate the time difference. And, it is common that a stacked trace has narrower bandwidth than the individual traces before stacking.

The effects of the forward and inverse equivalent offset mappings can be interpreted as a trace interpolation technique based on the scatter point model. In fact, some trace interpolation tools such as f-x predictive filter in Chan and Stewart (1996, 1997) are used to create reference data for residual statics analysis. Besides, migration and its inverse in general can be used as an interpolation tool.

### **APPLICATION TO BLACKFOOT DATA**

The geometry of the Blackfoot (CREWES Report, 1995) data is similar to the synthetic data used for the first experiment. There are 189 shots and 200 receivers. All the receivers were activated for each shot. So both the source fold and receiver fold are evenly high.

The data prepared for residual statics analysis had been processed by amplitude recovery, minimum phase spiking deconvolution followed by a time-variant spectrum whitening (TVSW), and then the refraction statics were applied. After a brute velocity analysis, the common shot stack and the common receiver stack are obtained from the data, and they are shown in Figure 21 and Figure 22. The static time shifts can be recognized, although they are not larger than 10 ms.

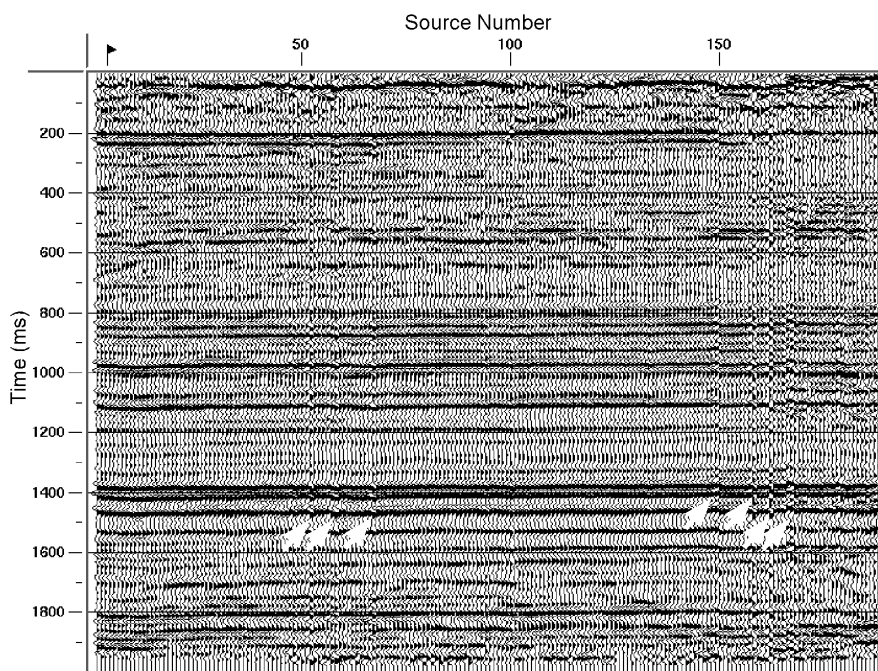


Figure 21: Brute common shot stack. The small white arrows indicate some locations where obvious statics problem occurs.

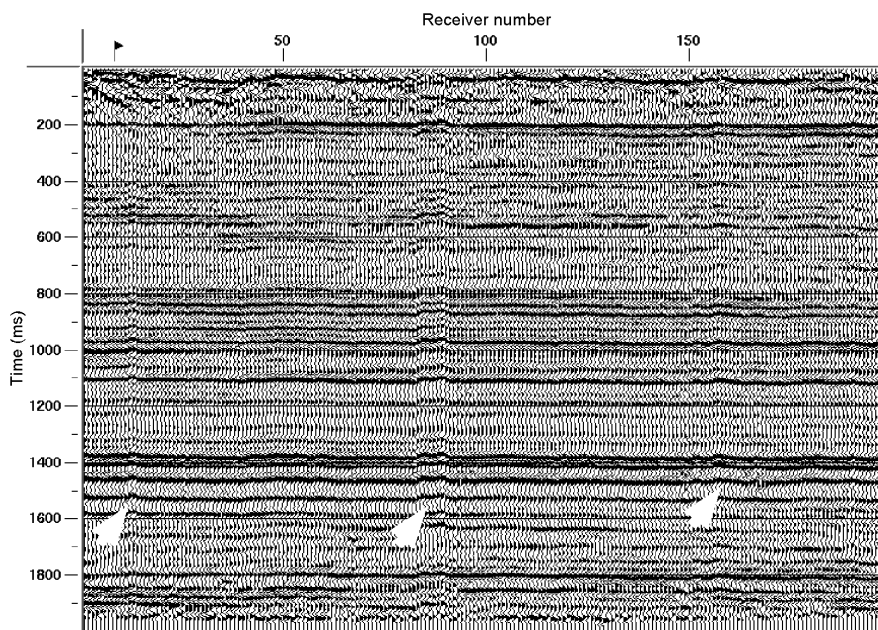


Figure 22: Brute common receiver stack. The white arrows indicate some locations where obvious statics problem occurs.

On the shot stack (Figure 21), the static time shift occurs at some individual locations (many are indicated by small white arrows) without evident continuities. While on the receiver stack, some static shifts happen in group (three of them are indicated by white arrows). So the receiver statics have some lower frequency contents than the source statics.

The statics problem can also be recognized on shot gathers. One shot gather before residual statics analysis is shown in Figure 23, and the some static shifts are indicated by white arrows. As a comparison, the reference gather created by asymptotic equivalent offset mappings is shown in Figure 24. The white arrows are put at the same places, but the static time shifts have been attenuated.

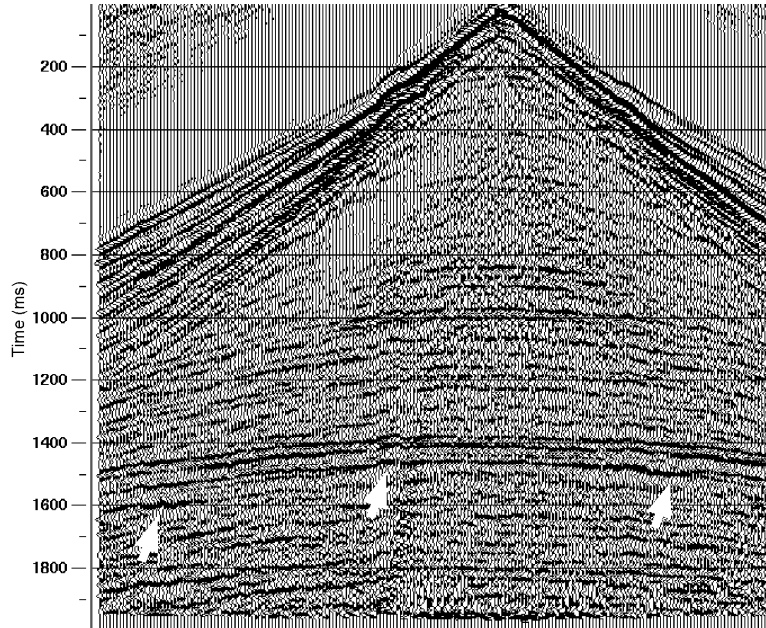


Figure 23: A shot gather with some recognizable static shifts. Some recognizable static time shifts are indicated. This shot gather is bandpass filtered and AGC-ed just for the display.

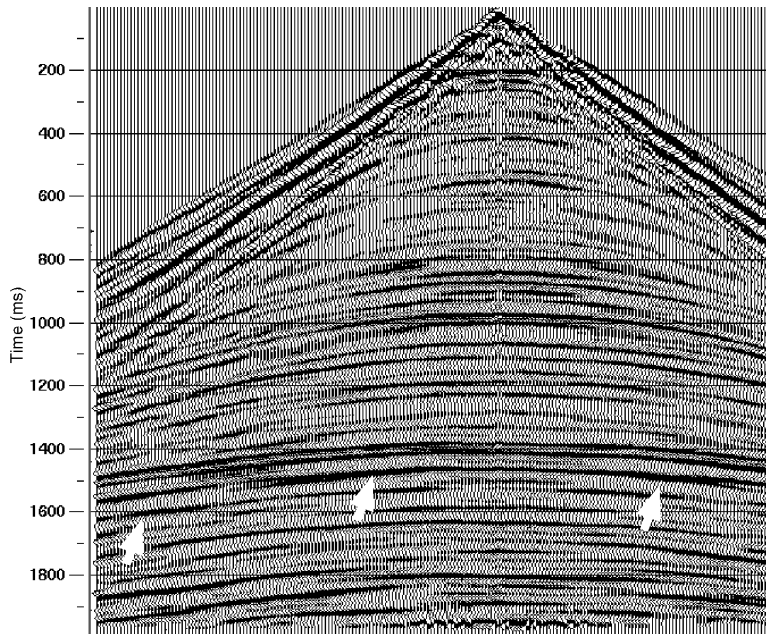


Figure 24: A shot gather extracted from the reference data created by asymptotic equivalent offset mapping. Comparing to the shot gather shown in Figure 23, the static shifts are attenuated.

Figure 25 and Figure 26 show the residual source statics and receiver statics respectively. The statics are estimated by using the reference data created by CSP method (one shot gather of the reference data is shown in Figure 24).

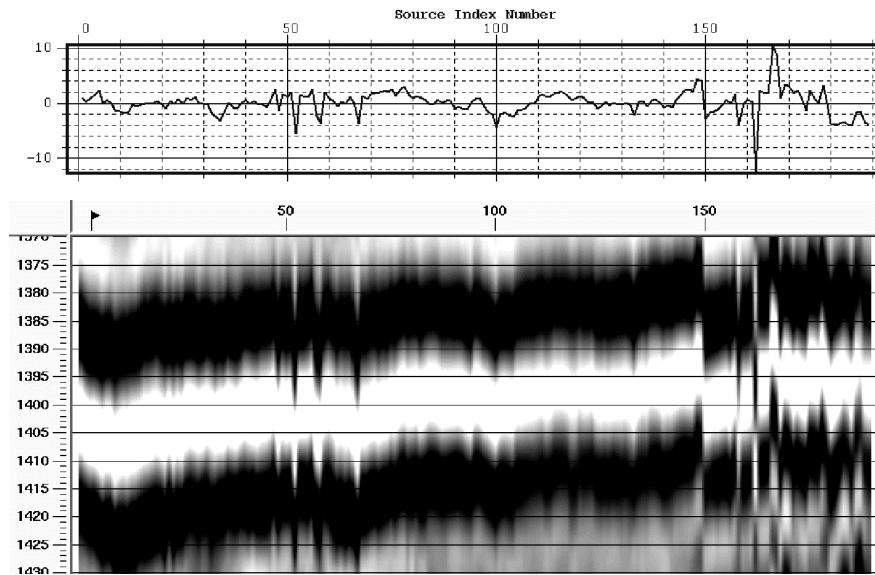


Figure 25: Residual shot statics estimated by CSP method, with the reference model data created by asymptotic equivalent offset mapping. The upper part shows the statics versus the source index number, while the lower part shows one major event on the brute common shot stack sections with time limited to 1370 ms to 1430 ms and the lateral position also indicated by source index numbers.

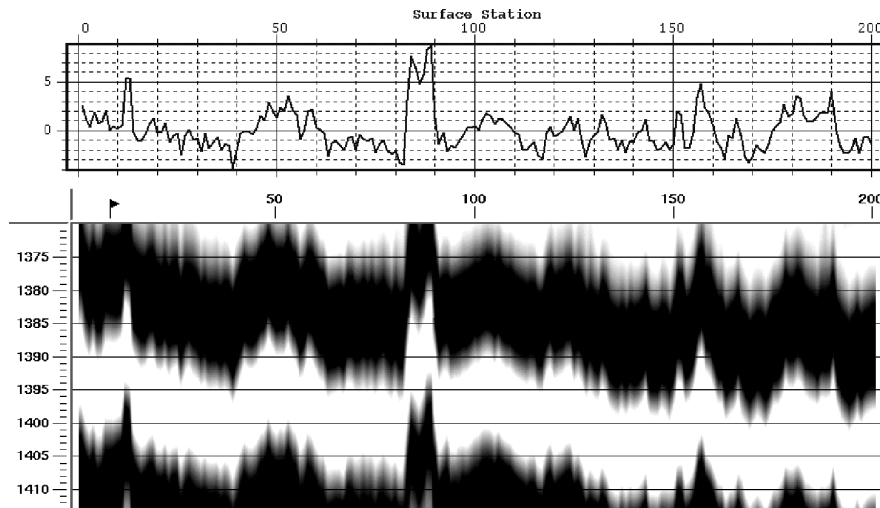


Figure 26: Residual receiver statics estimated by CSP method, with the reference model data created by asymptotic equivalent offset mapping. The upper part shows the statics versus the receiver surface location index number, while the lower part shows one major event on the brute common receiver stack section, with the lateral position also indicated by receiver surface location index numbers.

For comparison, one strong event in the brute common shot stack section (shown in Figure 21) and brute common receiver stack (shown in Figure 22) are zoomed and

aligned with the statics, and both statics and the sections are numbered by the same lateral position indices. The time shift of the event (shown in white) along the line has amazing matching with the estimated statics for both shot and receiver estimations.

The statics shown in Figure 25 and Figure 26 do improve the quality of the stack sections. At first, the common shot stack and the common receiver stack are obtained after a new set of stacking velocity is observed on the data after it is corrected by the statics shown in Figure 25 and Figure 26. The two stacks are shown in Figure 27 and Figure 28 respectively, where the improvement is recognizable comparing to the sections shown in Figure 21 and Figure 22.

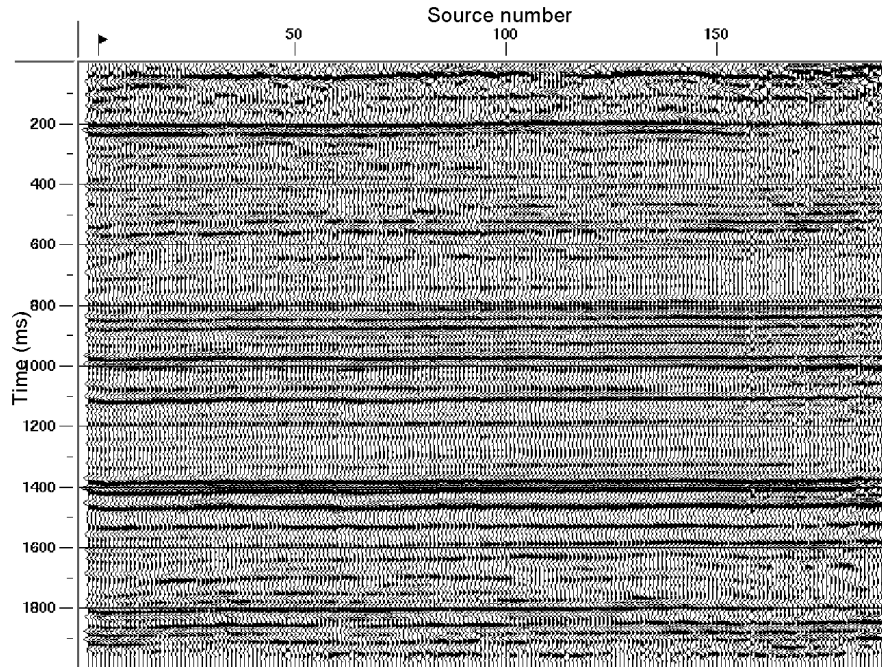


Figure 27: Common shot stack section after the residual statics estimated by CSP method are applied. The NMO velocity is also re-picked on the statics corrected data. Comparing to the brute common shot stack shown in Figure 21, the static time shifts are very well corrected.

The CMP stacked section is also improved after CSP statics applied, and new velocity is picked. But because of the size of the statics is small (less than 10 ms), it is difficult to find obvious differences on the whole CMP stacked sections from the brute stack section. However, detailed analysis shows improvements at almost any part of the stack, especially at the lower trace fold places. Figure 29 and figure 30 show two different parts of the three sections. The first section, shown as (a) in the figures, is the stack from the data before CSP statics applied and with the brute stacking velocity. The second section, shown as (b) in the figures, is the stack from the data without CSP statics but with a stacking velocity picked on CSP statics corrected data. The third section, shown as (c) in the figures, is the stack from the data with CSP statics with the velocity picked on this data. In general, the third section is the best, as expected.

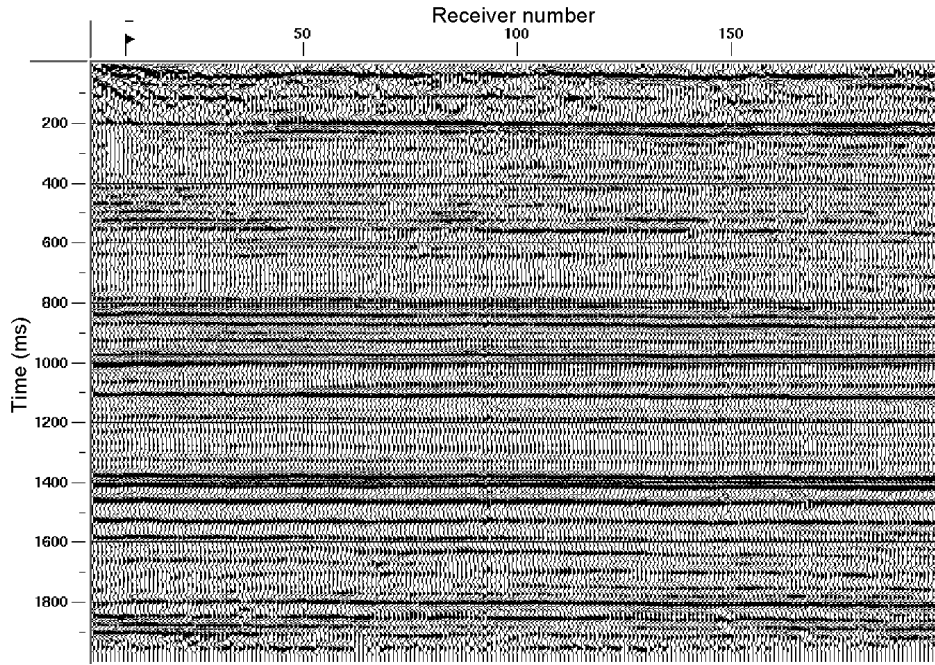


Figure 28: Common receiver stack section after the residual statics estimated by CSP method are applied. The NMO velocity is also re-picked on the statics corrected data. Comparing to the brute common receiver stack shown in Figure 22, the static time shifts are very well corrected.

Specifically, the shallower part of the CMP stacked section from CSP statics corrected data is improved more in the aspect of signal to noise ratio. The continuity of the shallow events is better almost every where in detail. Figure 29 is an example.

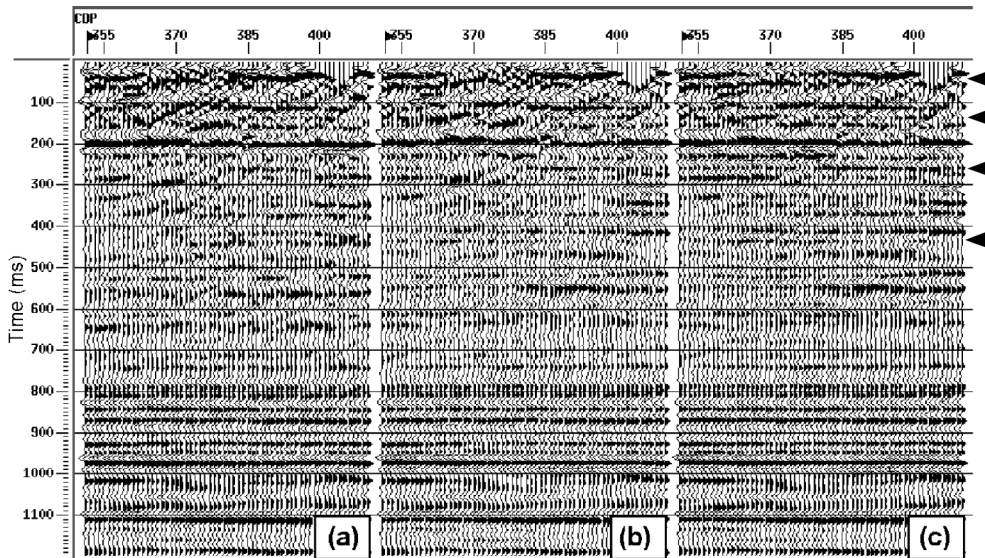


Figure 29: Comparison of three CMP stacked sections-at early times. (a) is part of the stack from the data before CSP statics applied and with the brute stacking velocity; (b) is part of the stack from the data without CSP statics but with a stacking velocity picked on CSP statics corrected data. (c) is part of the stack from the data with CSP statics with the velocity picked

on this data. The section in (c) is better than the other two almost anywhere, some are indicated by the small arrows.

On the other hand, residual static correction not only improves the signal to noise ratio, it also helps preserving high frequency content during the stacking process. Figure 30 shows some detail events indicated by arrows. They are between some stronger events, and if traveltime errors are significant or stacking velocity is not accurate enough, they may not be stacked as events at all.

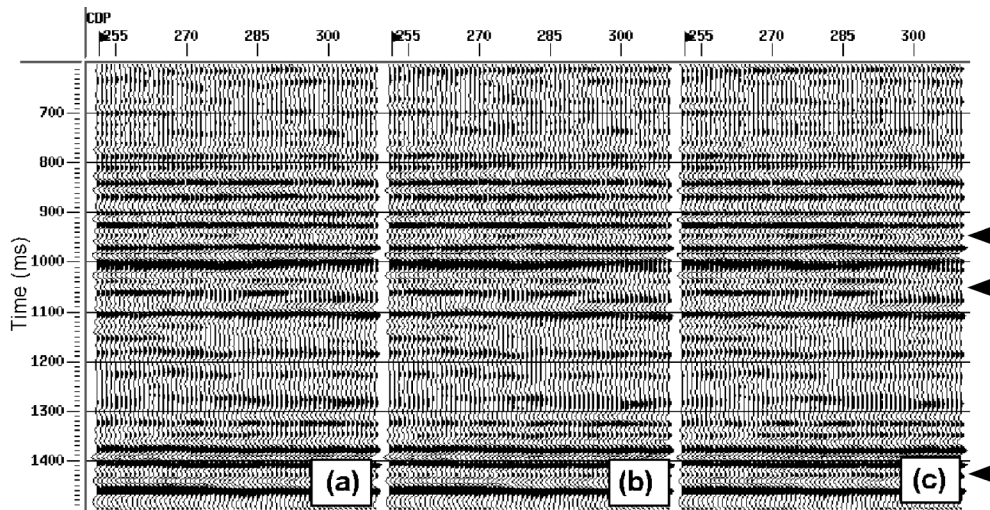


Figure 30: Comparison of three CMP stack sections-between strong events. (a) is part of the stack from the data before CSP statics applied and with the brute stacking velocity; (b) is part of the stack from the data without CSP statics but with a stacking velocity picked on CSP statics corrected data. (c) is part of the stack from the data with CSP statics with the velocity picked on this data. The three events arrow-pointed in (c) are clearer than their corresponding events in (a) and (b).

## CONCLUSIONS AND FUTURE WORK

The relation between prestack migration and residual statics can be as natural as the relation between NMO plus CMP stacking and residual statics analysis. If residual statics correction can be considered as the technique to obtain best possible stack section by reasonably removing some traveltime errors, it also can be designed as a technique to get the best possible prestack migration image.

The equivalent offset mapping introduced by EOM method is successfully used to form reference data for residual statics. This method can be used in the same way as conventional method, it also can be used when the velocity information is very difficult to observe because the complex subsurface structure.

Although this method involves some migration concepts, but practically, for the purpose of forming statics reference data, it can be very fast.

More experiments with this method are still needed, such as the application on complex structure data like Marmousi model and iterative convergence analysis. And,

more accurate amplitude consideration is needed in detail analysis. Some more efficient methods to do the cross-correlation and decomposition can still help.

This equivalent offset mapping method can be easily extended to 3D case, and with some changes, it can also be applied to converted-wave data statics analysis.

### **ACKNOWLEDGMENTS**

We thank the sponsors of the CREWES Project for their support. Dr. Wai-Kin Chan has given very helpful suggestions and discussions.

### **REFERENCES**

- Bancroft, J.C., and Geiger, H.D., 1995, Velocity sensitivity for equivalent offset prestack migration, CREWES Research Report, Vol.7.
- Bancroft, J.C., Geiger, H.D., Wang, S., Foltinek, D.S., 1995, Prestack migration by equivalent offset and CSP gathers: an update, CREWES Research Report, Vol. 7.
- Chan, W. and Stewart, R.R., 1996, f-x statics: CREWES Research Report, Vol.8.
- Chan, W. and Stewart, R.R., 1997, F-x statics for P-S seismic data, CREWES Research Report, Vol.9.
- Hileman, J.A., Embree, P., and Pflueger, J.C., 1968, Automatic static correction, *Geophysical Prospecting*, 16, 326-358
- Gardner, G.H.F., French, W.S. and Matzuk, T., 1974, Elements of migration and velocity analysis, *Geophysics*, 39, 811-825.
- Larner K., 1998, CSEG luncheon presentation, Calgary.
- Li, X. and Bancroft, J.C., 1997, Integrated residual statics analysis with prestack time migration, SEG Internat. Mtg., Expanded Abstract, Dallas, USA.
- Ronen, J., and Claerbout, J.F., 1985, Surface-consistent residual statics estimation by stack-power maximization, *Geophysics*, 50, 2759-2767
- Taner, M.T., Koehler, F., and Alhilali, A., 1974, Estimation and correction of near-surface time anomalies, *Geophysics*, 39, 441-463
- Wiggins, R.A., Larner, K.L., and Wisecup, R.D., 1976, Residual statics analysis as a general linear inverse problem, *Geophysics*, 41, 922-938.